THE JOURNAL OF PHYSICAL CHEMISTRY B

Article

Cite This: J. Phys. Chem. B 2019, 123, 3061−3067

pubs.acs.org/JPCB

High-Resolution ^{17}O NMR Spectroscopy of Structural Water

Eric G. Keeler,[†,‡,⊥] Vladimir K. Michaelis,[†,‡,#] Christopher B. Wilson,[‡,§,▽] Ivan Hung,[∥] Xiaoling Wang,[∥,▽] Zhehong Gan,[∥] and Robert G. Griffin*[,†,‡]

[†]Department of Chemistry, [‡]Francis Bitter Magnet Laboratory, and [§]Department of Physics, Massachusetts Institute of Technology, Cambridge, Massachusetts 02139 United States

[∥]National High Magnetic Field Laboratory, Florida State University, Tallahassee, Florida 32310, United States

Supporting Information

ABSTRACT: The importance of studying site-specific interactions of structurally similar water molecules in complex systems is well known. We demonstrate the ability to resolve four distinct bound water environments within the crystal structure of lanthanum magnesium nitrate hydrate via ^{17}O solid state nuclear magnetic resonance (NMR) spectroscopy. Using high-resolution multidimensional experiments at high magnetic fields (18.8−35.2 T), each individual water environment was resolved. The quadrupole coupling constants and asymmetry parameters of the ^{17}O of each water were determined to be between 6.6 and 7.1 MHz, 0.83 and 0.90, respectively. The resolution of the four unique, yet similar, structural waters within a hydrated crystal via ^{17}O NMR spectroscopy demonstrates the ability to decipher the unique electronic environment of structural water within a single hydrated crystal structure.

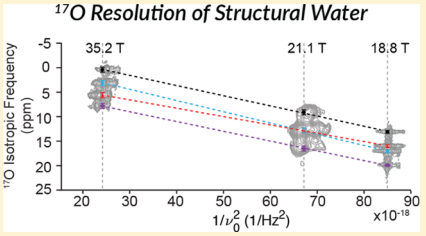

INTRODUCTION

The influence of water on the structure, stability, function, and dynamics of complex biological and inorganic systems underlines the importance of understanding the detailed structure of individual water molecules in such systems.[1] For example, it is well known that water is intimately involved in the intra- and intermolecular hydrogen bonding of proteins, membranes, and nucleic acids[2−4] and is therefore important in determining the secondary and tertiary structures of these macromolecular systems. Recently, in a combined cryo-electron microscopy and magic-angle spinning (MAS) NMR study of the structure of amyloid fibrils from our group, we observed a water bilayer that is thought to be essential for stabilizing the structure of the paired twisted β-sheets.[5−10] In addition to the impact of water on the structure of biochemical systems, water is known to influence other systems,[11−19] one such system, in particular, is the formation of organic rosette nanotubes.[18,19] These and other results have stimulated the study of the structure of water in multiple different systems using solid state NMR[10,19−27] with many studies focusing on the mobile waters of hydration. However, the resolution of different water molecules, and therefore the site-specific study of these waters, has proved challenging because of the small chemical shift range present in ^{1}H NMR spectra which is the primary probe of the water molecules.[10,20−25] In contrast, the sizeable chemical shift range (~2000 ppm) and quadrupolar nature of ^{17}O (I = 5/2) make it attractive for the study of intra- and intermolecular hydrogen bonding interactions involving water. However, ^{17}O NMR is inherently insensitive due to the low natural abundance (~0.037%) and a small gyromagnetic ratio (~1/7th of ^{1}H). In addition, ^{17}O NMR spectra are broadened by the second-order quadrupolar interaction which is not averaged by MAS.[28] Despite these shortcomings, ^{17}O has been used extensively to study biological and inorganic systems, by utilizing isotopic enrichment[29−33] and high magnetic field strengths (≥16.4 T).[34−39] Approaches improving the resolution of ^{17}O MAS NMR spectra by attenuating the second-order quadrupolar interaction, such as multiple quantum MAS (MQMAS)[40] and satellite transition MAS (STMAS),[41] have been shown to yield well-resolved isotropic quadrupolar spectra. And, despite the poor efficiency (~5%) of these techniques in the presence of large quadrupole coupling constants (>5 MHz),[42,43] they have been used to successfully study ^{17}O-enriched biological samples and produced promising results.[44−47] For example, the increased resolution that is present in the MQMAS experiment allowed studies of inorganic glasses and minerals that could not be achieved with traditional MAS experiments.[32,33,48−58]

In recent studies of $H_2{}^{17}O$ structurally bound to organic and inorganic crystals,[11,59,60] we observed ^{17}O chemical shifts dispersed over ~50 ppm. This result suggests that ^{17}O NMR can be used to distinguish bound water in complex biological and inorganic systems via the dispersion of oxygen chemical shifts. Here, we report ^{17}O spectra of lanthanum magnesium nitrate hydrate [$La_2Mg_3(NO_3)_{12}\cdot 24H_2{}^{17}O$] (LMN), a hydrated crystal containing four distinct water environments (each environment is comprised of six individual, yet equivalent, waters),[61] as a model system that demonstrates this possibility. As illustrated in Figure 1, each of the three Mg^{2+} ions is coordinated to six water molecules, and the remaining waters in the crystal exist in a layer between the lanthanum nitrate and

Received: March 11, 2019
Published: March 18, 2019

Downloaded via FLORIDA STATE UNIV on September 3, 2020 at 14:04:20 (UTC).
See https://pubs.acs.org/sharingguidelines for options on how to legitimately share published articles.

ACS Publications © 2019 American Chemical Society

DOI: 10.1021/acs.jpcb.9b02277
J. Phys. Chem. B 2019, 123, 3061−3067

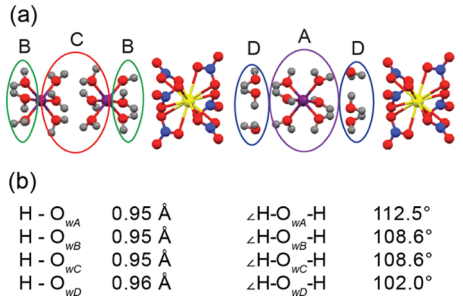

Figure 1. LMN crystal structure (a) showing the four crystallographically distinct water environments labeled as A–D and corresponding (b) interatomic distances and angles determined by neutron diffraction.[61]

one of the magnesium hydrate subunits. The four crystallographically distinct waters are indicated on the molecular unit in Figure 1a with the average O–H bond distance and ∠HOH angle for each water site given in Figure 1b.

EXPERIMENTAL SECTION

Materials and Synthesis. Lanthanum magnesium nitrate hydrate, $La_2Mg_3(NO_3)_{12}{\cdot}24H_2{}^{17}O$, samples were synthesized by dissolving lanthanum nitrate hexahydrate, $La(NO_3)_3{\cdot}6H_2O$ (Sigma Aldrich (SA), St. Louis, MO), and magnesium nitrate hexahydrate, $Mg(NO_3)_2{\cdot}6H_2O$ (SA), in excess ^{17}O-labeled water (90% $H_2{}^{17}O$, Cambridge Isotopes Laboratories (CIL), Andover, MA), and recrystallizing in a sealed eppendorf tube over the course of 2–14 days. The crystals were then air-dried and ground into a fine powder using an agate mortar and pestle.

Nuclear Magnetic Resonance Spectroscopy. Oxygen-17 NMR experiments were performed at 18.8 (Francis Bitter Magnet Laboratory – Massachusetts Institute of Technology, FBML-MIT), 18.8 (National High Magnetic Field Laboratory, NHMFL), and 21.1 (FBML-MIT) T using a Bruker Avance II or III spectrometer. Oxygen-17 NMR experiments were also performed at 35.2 T on the series-connected hybrid magnet at the NHMFL using a Bruker Avance NEO console and a single-resonance 3.2 mm MAS probe designed and constructed at the NHMFL.[62] A recycle delay of between 0.5 and 1 s was used for all ^{17}O experiments, unless otherwise noted. Between 2400 and 8192 scans with $\gamma B_1/2\pi$ (^{17}O) = 27.7–140 kHz were utilized for ^{17}O MAS NMR experiments. A spinning frequency ($\omega_R/2\pi$) of between 10 and 23 kHz was used for ^{17}O MAS experiments at 18.8, and 21.1 T, respectively. One-dimensional MAS NMR experiments were acquired using a Hahn-echo ($\pi/2-\tau-\pi-\tau-$acquire) pulse sequence.

Two-dimensional ^{17}O-shifted echo triple quantum magic-angle spinning (3QMAS) spectra were acquired at 18.8, 21.1, and 35.2 T with 128, 92, 44 (80) rotor-synchronized t_1 increments with increments of 62.5, 43.48, and 100 μs with 2016, 2400, and 1152 (960) scans and $\omega_R/2\pi$ = 16, 23, and 10 kHz. The 3QMAS experiments at 18.8 and 35.2 T were performed with 3Q excitation and conversion pulses of 3 and 1 μs ($\gamma B_1/2\pi$ = 100 kHz) and $\pi/2$ and π pulses of 2.5 and 5 μs ($\gamma B_1/2\pi$ = 33.3 kHz). The 3QMAS experiments at 21.1 T were performed with 3Q excitation and conversion pulses of 4.6 and 2.8 μs ($\gamma B_1/2\pi$ = 27.7 kHz) and $\pi/2$ and π pulses of 3 and 6 μs ($\gamma B_1/2\pi$ = 27.7 kHz). Spectra were referenced to liquid water, ^{17}O (18% $H_2{}^{17}O$, 0 ppm), via the substitution method.[63]

Spectral Processing and Simulations. All spectra were processed by RNMR (Dr. D. Ruben, FBML-MIT), TOPSPIN (Bruker, Billerica), or MATLAB (MathWorks, Natick, MA) with between 10 and 500 Hz of exponential apodization. ^{17}O spectral simulations were performed using either the WSolids,[64] DMFit,[65] or SIMPSON[66] software packages.

RESULTS AND DISCUSSION

At high magnetic fields (18.8, 21.1, and 35.2 T[62]), multiple unique bound water environments were identified by ^{17}O NMR spectroscopy of a crystalline sample of LMN prepared from $H_2{}^{17}O$. The 3QMAS spectra illustrated in Figure 2 reveal

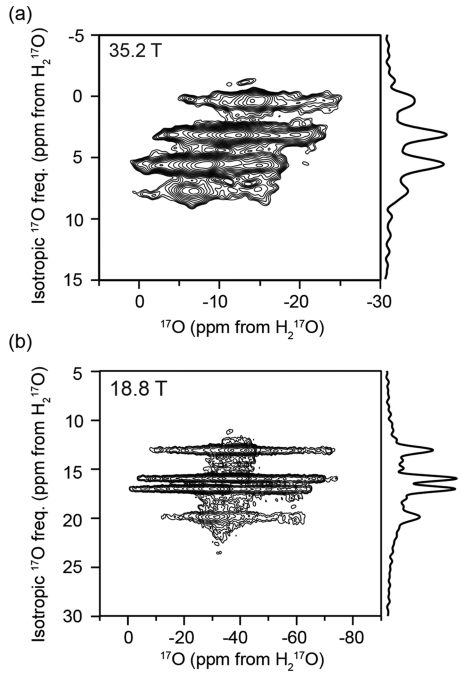

Figure 2. Oxygen-17 2D MQMAS NMR spectra at (a) 35.2 T ($\omega_{0H}/2\pi$ = 1500 MHz) and (b) 18.8 T ($\omega_{0H}/2\pi$ = 800 MHz). Four distinct water sites are resolved in each spectrum. The projection of the isotropic dimension is shown to the right of each spectrum.

four resolved peaks in the 2D landscape corresponding to four unique bound waters within the LMN crystals. The projection of the isotropic dimension at 18.8 T was found to have an integrated intensity ratio of 1:1:1:1 for the four environments (Figure 3) suggesting that they are the same bound water species that were identified by neutron diffraction.[61] The observed isotropic frequency of the MQMAS spectrum is a linear combination of the isotropic chemical shift and the 2nd order quadrupolar shift. However, the observed isotropic frequency of the ^{17}O 3QMAS experiment is given by the equation[44]

$$\delta_{iso} = \delta_{3Q} + \frac{3}{850}\frac{P_Q^2}{\nu_0^2} \times 10^{-6}$$

where

$$P_Q = C_Q\sqrt{1 + \frac{\eta^2}{3}}$$

resulting in a change in the relative isotropic frequencies in spectra recorded at different static magnetic fields (Figure 4).

DOI: 10.1021/acs.jpcb.9b02277
J. Phys. Chem. B 2019, 123, 3061–3067

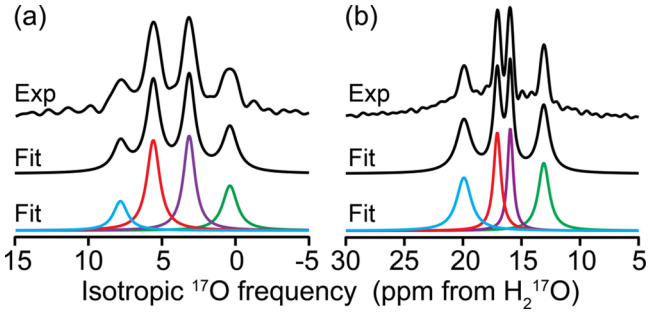

Figure 3. Experimental and fit isotropic projections of ^{17}O 2D MQMAS spectra at (a) 35.2 T ($\omega_{0H}/2\pi$ = 1500 MHz) and (b) 18.8 T ($\omega_{0H}/2\pi$ = 800 MHz). Four distinct water environments are resolved with isotropic frequencies of (a) 0.4 ± 1, 3.1 ± 1, 5.6 ± 1, and 7.8 ± 1 ppm and (b) 13.1 ± 1, 16.0 ± 1, 17.1 ± 1, and 19.9 ± 1 ppm. The Lorenztian fits of each environment indicate a ratio of populations of 1:1:1:1.

There are also differences in the breadth of the peaks in the isotropic dimension that could arise from differences in structural heterogeneity or T_2 relaxation arising from the molecular motions (2-fold flips) of the different water environments.

The resolution of multiple water environments with such a small chemical shift difference demonstrates the ability to use ^{17}O NMR to study bound water in complex systems where the water environments are expected to be similar. The MQMAS spectrum at 21.1 T, Figure S1, shows only three resolved peaks. The field dependence of the 2nd order quadrupolar shift causes the two center peaks, which are resolved at 18.8 and 35.2 T, to be nearly indistinguishable at 21.1 T (Figure 4). The determined ratio of the three peaks is 1:2:1, which is expected considering that the center peak is two unresolved water environments. Using iterative spectral simulations of the 3Q-filtered MAS lineshape of each of the four peaks, the electric field gradient (EFG) and chemical shift anisotropy (CSA) tensor parameters were determined and are given in Table 1.

The breadth and asymmetry of the second-order quadrupolar lineshape of the central transition of half-integer quadrupolar nuclei, as measured by the quadrupole coupling constant, C_Q, and the asymmetry parameter, η_Q, depend on the local structure of the oxygen nucleus. Therefore, the differences in the EFG and CSA tensor parameters could yield a better understanding of the structure of each of the water environments.

The quadrupole coupling constants were found to be between 6.6 and 7.1 MHz. Previous work has shown that the asymmetry parameter, η_Q, is a sensitive indicator of the HOH bond angle[67] and therefore useful for characterizing individual water molecules. However, in the case of LMN the fast limit 2-fold flipping of the bound water at room temperature averages the EFG tensor.[11,59,60] This limits the utility of the asymmetry parameter in distinguishing different water environments. The experimentally determined asymmetry parameters for the four water environments in LMN were found to be between 0.83 and 0.9. The differences found in the EFG tensors likely reflect both differences in the local structure and the room temperature dynamics of the bound waters. Both the EFG and CSA tensor values were found to be in good agreement with previous results for bound water within hydrated crystals.[11,59,60] Although the one-dimensional MAS NMR spectra at 18.8 and 21.1 T (Figure 5) indicated the presence of multiple unique oxygen environments, the 2D MQMAS experiments were necessary to identify and characterize the four oxygen environments (Figures 2 and 5). Although inclusion of the ^{17}O chemical shift parameters did not affect the 1D MAS NMR lineshape, it was necessary to include the CSA tensor parameters (Table 1) for the simulations of the 3QMAS lineshapes at 35.2 T (Figure 6). The 3QMAS

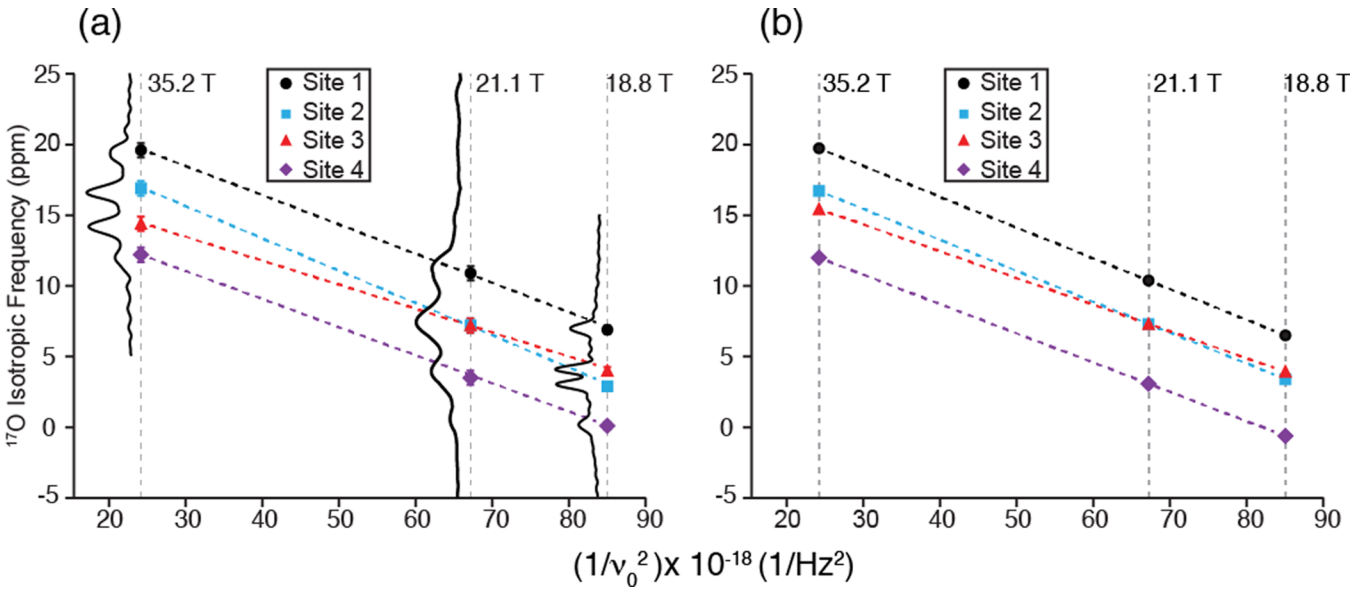

Figure 4. Magnetic field dependence (B_o = 18.1−35.2 T) of the observed ^{17}O isotropic frequency shown using the (a) observed isotropic frequency from the 2D MQMAS spectra, and (b) using the equation: $\delta_{iso} = \delta_{3Q} + \frac{3}{850}\frac{P_Q^2}{\nu_0^2} \times 10^{-6}$, where $P_Q = C_Q\sqrt{1+\frac{\eta^2}{3}}$ and ν_0 is the Larmor frequency of ^{17}O and is calculated from the values in Table 1. A projection of the isotropic dimension at each field is shown to the left of the isotropic frequencies for each field in (a). The dashed lines (black, red, blue, and purple) are linear fitted lines to the isotropic frequencies of each site.

DOI: 10.1021/acs.jpcb.9b02277
J. Phys. Chem. B 2019, 123, 3061−3067

Table 1. ^{17}O EFG and CSA Tensor Parameters Determined from MAS and MQMAS NMR[a]

^{17}O site	C_Q (±0.3) (MHz)	η_Q (±0.15)	δ_{iso} (ppm)	Ω (±30) (ppm)	κ (±0.5)	δ_{3Q} (±0.25) (ppm) at 18.8 T	δ_{3Q} (±0.5) (ppm) at 21.1 T	δ_{3Q} (±0.5) (ppm) at 35.2 T
1	7.1	0.8_5	−5 ± 2	50	−1	13.1	8.9	0.4
2	7.1	0.8_3	−2 ± 2	70	−1	17.1	nr	3.1
3	6.6	0.8_3	0 ± 2	70	−1	16.0	nr	5.6
4	6.8	0.9	3 ± 2	80	−1	19.9	16.3	7.8

[a]nr: not resolved, one peak at 12.6 ± 0.5 ppm.

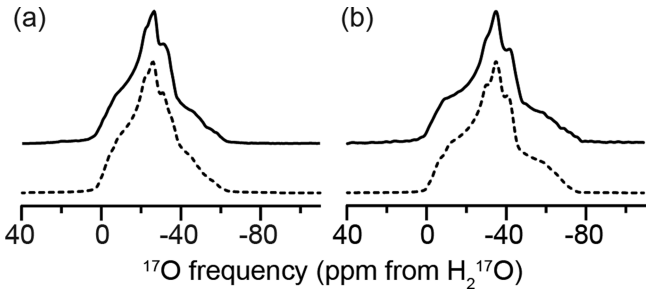

Figure 5. Experimental (solid) and simulated (dashed) ^{17}O MAS NMR spectra at (a) 21.1 T ($\omega_{0H}/2\pi$ = 900 MHz) and (b) 18.8 T ($\omega_{0H}/2\pi$ = 800 MHz) with $\omega_R/2\pi$ = 23, and 20 kHz, respectively. EFG tensor parameters for the spectral simulations are given in Table 1.

dimension was analyzed from the projection of the direct dimension of the 2D MQMAS experiment.

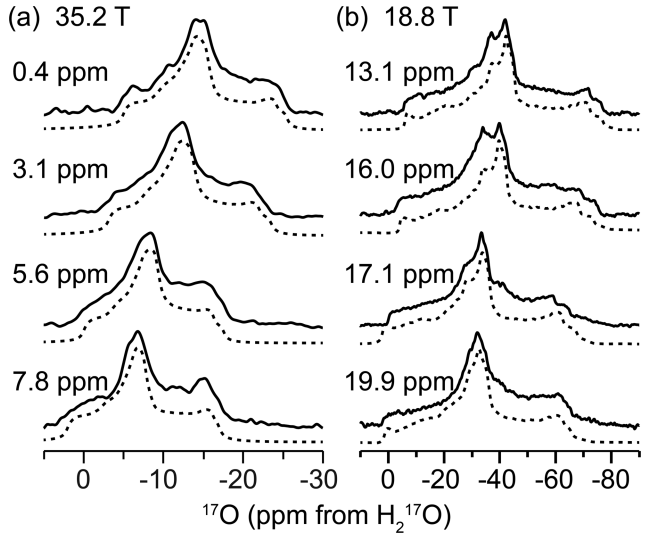

Figure 6. Projections of the 3Q-filtered lineshape of each ^{17}O resonance from Figure 2 at (a) 35.2 T ($\omega_{0H}/2\pi$ = 1500 MHz) and (b) 18.8 T ($\omega_{0H}/2\pi$ = 800 MHz) with spectral simulations displayed as dashed lines. The EFG and CSA tensor parameters of the simulations are given in Table 1.

Unique assignments of the NMR resolved peaks to the crystal structure water environments were not performed in this study due to the complex dynamics of such environments.[11,59,60,68−70] The librational modes of the bound water sites have been shown to average the EFG tensors and, therefore, complicate the relationship between local and hydrogen bonding structure and the experimentally determined EFG tensors at room temperature. Although a dependence of the isotropic chemical shift and the OH bond distance and ∠HOH bond angle was reported in crystalline amino acid and dipeptide hydrates,[60] a study of crystalline inorganic hydrates did not demonstrate the same dependence.[11] Either correlation spectroscopy between the ^{17}O and nearby nuclei or low-temperature NMR could be utilized to assist in determining which NMR environments correspond to their neutron diffraction counterparts.

CONCLUSIONS

Notwithstanding a unique assignment of the $H_2{}^{17}O$ lines, the resolution of multiple structurally similar environments indicates the benefit of high magnetic fields for the study of structurally important bound water. Due to the nature of the crystal structure studied here, correlation spectroscopy (e.g., ^{13}C-^{17}O, ^{15}N-^{17}O)[47,71−74] was not performed to better identify the oxygen environments that were resolved. However, for complex biological systems, such as GNNQQNY or $TTR_{105-115}$,[6−9] where more accessible correlation spectroscopy is available, an identification of resolved structural water molecules may be possible. The ability to use high-resolution ^{17}O MAS NMR to study unique, yet similar, structural waters in a single inorganic crystal structure indicates the possibility of analyzing structural waters in complex inorganic and biological systems. The addition of dynamic nuclear polarization to the high-resolution ^{17}O MAS NMR[71,72,75,76] will enhance the ability to study the small number of structural water molecules in these complex systems in comparison to the inorganic crystal in this study.

ASSOCIATED CONTENT

Supporting Information

The Supporting Information is available free of charge on the ACS Publications website at DOI: 10.1021/acs.jpcb.9b02277.

Additional Figures S1−S4: Experimental (a) ^{17}O 2D MQMAS spectrum, and experimental (b) and fit (c, d) isotropic projections of the ^{17}O 2D MQMAS spectrum at 21.1 T; Experimental (a) ^{17}O 2D MQMAS spectrum, and experimental (b) and fit (c, d) isotropic projections of the ^{17}O 2D MQMAS spectrum at 35.2 T; oxygen-17 2D MQMAS NMR spectrum at 21.1 T ($\omega_{0H}/2\pi$ = 900 MHz) with $\gamma B_1/2\pi$ = 100 kHz continuous-wave ^{1}H decoupling; simulated ^{17}O MAS NMR spectra at 16.4−35.2 T (700−1500 MHz, ^{1}H NMR) and the projection of the direct 3QMAS dimension (PDF)

AUTHOR INFORMATION

Corresponding Author

*E-mail: rgg@mit.edu.

ORCID

Eric G. Keeler: 0000-0002-9598-7148
Vladimir K. Michaelis: 0000-0002-6708-7660
Robert G. Griffin: 0000-0003-1589-832X

DOI: 10.1021/acs.jpcb.9b02277
J. Phys. Chem. B 2019, 123, 3061−3067

Present Addresses

[▽]Department of Physics, University of California, Santa Barbara, Santa Barbara, California 93160, United States (C.B.W. and X.W.).

[#]Department of Chemistry, University of Alberta, Edmonton, Alberta, T6G 2G2 Canada (V.K.M.).

[⊥]Department of Chemistry, Columbia University, New York, New York 10027, United States (E.G.K.).

Funding

No competing financial interests have been declared.

Notes

The authors declare no competing financial interest.

■ ACKNOWLEDGMENTS

This work was supported by the National Institutes of Health (NIH) through grant numbers: AG058504 and EB002026. V.K.M. is grateful to the Natural Sciences and Engineering Research Council of Canada and the Government of Canada for a Banting Postdoctoral Fellowship. Part of the work was performed at the National High Magnetic Field Laboratory supported through National Science Foundation Cooperative Agreement (DMR-1644779) and by the State of Florida. The development of the 35.2 T magnet and NMR instrumentation was supported by National Science Foundation DMR-1039938 and DMR-0603042.

■ REFERENCES

(1) Levy, Y.; Onuchic, J. N. Water and proteins: A love-hate relationship. *Proc. Natl. Acad. Sci. USA* **2004**, *101*, 3325−3326.

(2) Głowacki, E. D.; Irimia-Vladu, M.; Bauer, S.; Sariciftci, N. S. Hydrogen-bonds in molecular solids - from biological systems to organic electronics. *J. Mater. Chem. B* **2013**, *1*, 3742−3753.

(3) Horowitz, S.; Trievel, R. C. Carbon-Oxygen Hydrogen Bonding in Biological Structure and Function. *J. Biol. Chem.* **2012**, *287*, 41576−41582.

(4) Griffin, R. G. Observation of the effect of water on the phosphorus-31 nuclear magnetic resonance spectra of dipalmitoyllecithin. *J. Am. Chem. Soc.* **1976**, *98*, 851−853.

(5) Caporini, M. A.; Bajaj, V. S.; Veshtort, M.; Fitzpatrick, A.; MacPhee, C. E.; Vendruscolo, M.; Dobson, C. M.; Griffin, R. G. Accurate Determination of Interstrand Distances and Alignment in Amyloid Fibrils by Magic Angle Spinning NMR. *J. Phys. Chem. B* **2010**, *114*, 13555−13561.

(6) Debelouchina, G. T.; Bayro, M. J.; Fitzpatrick, A. W.; Ladizhansky, V.; Colvin, M. T.; Caporini, M. A.; Jaroniec, C. P.; Bajaj, V. S.; Rosay, M.; MacPhee, C. E.; et al. Higher Order Amyloid Fibril Structure by MAS NMR and DNP Spectroscopy. *J. Am. Chem. Soc.* **2013**, *135*, 19237−19247.

(7) Debelouchina, G. T.; Bayro, M. J.; van der Wel, P. C. A.; Caporini, M. A.; Barnes, A. B.; Rosay, M.; Maas, W. E.; Griffin, R. G. Dynamic nuclear polarization-enhanced solid-state NMR spectroscopy of GNNQQNY nanocrystals and amyloid fibrils. *Phys. Chem. Chem. Phys.* **2010**, *12*, 5911−5919.

(8) Fitzpatrick, A. W. P.; Debelouchina, G. T.; Bayro, M. J.; Clare, D. K.; Caporini, M. A.; Bajaj, V. S.; Jaroniec, C. P.; Wang, L.; Ladizhansky, V.; Müller, S. A.; et al. Atomic structure and hierarchical assembly of a cross-β amyloid fibril. *Proc. Natl. Acad. Sci. USA* **2013**, *110*, 5468−5473.

(9) van der Wel, P. C. A.; Hu, K. N.; Lewandowski, J.; Griffin, R. G. Dynamic nuclear polarization of amyloidogenic peptide nanocrystals: GNNQQNY, a core segment of the yeast prion protein Sup35p. *J. Am. Chem. Soc.* **2006**, *128*, 10840−10846.

(10) Wang, T.; Jo, H.; DeGrado, W. F.; Hong, M. Water Distribution, Dynamics, and Interactions with Alzheimer's beta-Amyloid Fibrils Investigated by Solid-State NMR. *J. Am. Chem. Soc.* **2017**, *139*, 6242−6252.

(11) Nour, S.; Widdifield, C. M.; Kobera, L.; Burgess, K. M. N.; Errulat, D.; Terskikh, V. V.; Bryce, D. L. Oxygen-17 NMR spectroscopy of water molecules in solid hydrates. *Can. J. Chem.* **2016**, *94*, 189−197.

(12) Bell, D. R.; Rossman, G. R. Water in Earths Mantle - the Role of Nominally Anhydrous Minerals. *Science* **1992**, *255*, 1391−1397.

(13) Benziger, J.; Bocarsly, A.; Cheah, M. J.; Majsztrik, P.; Satterfield, B.; Zhao, Q. Mechanical and Transport Properties of Nafion: Effects of Temperature and Water Activity. *Fuel Cells Hydrogen Storage* **2011**, *141*, 85−113.

(14) Bobylev, I. B.; Gerasimov, E. G.; Zyuzeva, N. A. Effect of structural water on the critical characteristics of highly textured $YBa_2Cu_3O_{6.9}$. *Phys. Solid State* **2014**, *56*, 1742−1747.

(15) Lebofsky, L. A.; Feierberg, M. A.; Tokunaga, A. T.; Larson, H. P.; Johnson, J. R. The 1.7- to 4.2-μm Spectrum of Asteroid 1 Ceres - Evidence for Structural Water in Clay-Minerals. *Icarus* **1981**, *48*, 453−459.

(16) Xu, W. Q.; Hausner, D. B.; Harrington, R.; Lee, P. L.; Strongin, D. R.; Parise, J. B. Structural water in ferrihydrite and constraints this provides on possible structure models. *Am. Mineral.* **2011**, *96*, 513−520.

(17) Zhao, Q. A.; Majsztrik, P.; Benziger, J. Diffusion and Interfacial Transport of Water in Nafion. *J. Phys. Chem. B* **2011**, *115*, 2717−2727.

(18) Yamazaki, T.; Fenniri, H.; Kovalenko, A. Structural Water Drives Self-assembly of Organic Rosette Nanotubes and Holds Host Atoms in the Channel. *Chemphyschem* **2010**, *11*, 361−367.

(19) Fenniri, H.; Tikhomirov, G. A.; Brouwer, D. H.; Bouatra, S.; El Bakkari, M.; Yan, Z. M.; Cho, J. Y.; Yamazaki, T. High Field Solid-State NMR Spectroscopy Investigation of ^{15}N-Labeled Rosette Nanotubes: Hydrogen Bond Network and Channel-Bound Water. *J. Am. Chem. Soc.* **2016**, *138*, 6115−6118.

(20) Lesage, A.; Böckmann, A. Water-protein interactions in microcrystalline Crh measured by ^{1}H-^{13}C solid-state NMR spectroscopy. *J. Am. Chem. Soc.* **2003**, *125*, 13336−13337.

(21) Lesage, A.; Emsley, L.; Penin, F.; Böckmann, A. Investigation of dipolar-mediated water-protein interactions in microcrystalline Crh by solid-state NMR spectroscopy. *J. Am. Chem. Soc.* **2006**, *128*, 8246−8255.

(22) Luo, W. B.; Hong, M. Conformational Changes of an Ion Channel Detected Through Water-Protein Interactions Using Solid-State NMR Spectroscopy. *J. Am. Chem. Soc.* **2010**, *132*, 2378−2384.

(23) Sergeyev, I. V.; Bahri, S.; Day, L. A.; McDermott, A. E. Pf1 bacteriophage hydration by magic angle spinning solid-state NMR. *J. Chem. Phys.* **2014**, *141*, No. 12B641_1.

(24) White, P. B.; Wang, T.; Park, Y. B.; Cosgrove, D. J.; Hong, M. Water-Polysaccharide Interactions in the Primary Cell Wall of Arabidopsis thaliana from Polarization Transfer Solid-State NMR. *J. Am. Chem. Soc.* **2014**, *136*, 10399−10409.

(25) Mandala, V. S.; Gelenter, M. D.; Hong, M. Transport-Relevant Protein Conformational Dynamics and Water Dynamics on Multiple Time Scales in an Archetypal Proton Channel: Insights from Solid-State NMR. *J. Am. Chem. Soc.* **2018**, *140*, 1514−1524.

(26) Shi, L. C.; Kawamura, I.; Jung, K. H.; Brown, L. S.; Ladizhansky, V. Conformation of a Seven-Helical Transmembrane Photosensor in the Lipid Environment. *Angew. Chem., Int. Ed.* **2011**, *50*, 1302−1305.

(27) Wilson, E. E.; Awonusi, A.; Morris, M. D.; Kohn, D. H.; Tecklenburg, M. M. J.; Beck, L. W. Three structural roles for water in bone observed by solid-state NMR. *Biophys. J.* **2006**, *90*, 3722−3731.

(28) Grandinetti, P. J.; Trease, N. M.; Ash, J. T. Symmetry Pathways in Solid State NMR. *Prog. Nucl. Magn. Reson. Spectrosc.* **2011**, *59*, 121−196.

(29) Wong, A.; Poli, F. Solid-State ^{17}O NMR Studies of Biomolecules. *Annual Reports on NMR Spectroscopy*; Academic Press, 2014; Vol. 83, pp 145−220.

(30) Wu, G. Solid-State ^{17}O NMR Studies of Organic and Biological Molecules. *Prog. Nucl. Magn. Reson. Spectrosc.* **2008**, *52*, 118−169.

DOI: 10.1021/acs.jpcb.9b02277
J. Phys. Chem. B 2019, 123, 3061−3067

(31) Wu, G., Oxygen 17 NMR Studies of Organic and Biological Molecules. In *eMagRes*; John Wiley & Sons, Ltd.: Chichester, UK, 2011.
(32) Ashbrook, S. E.; Smith, M. E. Solid state ^{17}O NMR - An introduction to the background principles and applications to inorganic materials. *Chem. Soc. Rev.* **2006**, *35*, 718−735.
(33) Ashbrook, S. E.; Smith, M. E. Oxygen-17 NMR of Inorganic Materials. In *eMagRes*; John Wiley & Sons, Ltd: Chichester, UK, 2007.
(34) Aguiar, P. M.; Michaelis, V. K.; McKinley, C. M.; Kroeker, S. Network connectivity in cesium borosilicate glasses: ^{17}O multiple-quantum MAS and double-resonance NMR. *J. Non-Cryst. Solids* **2013**, *363*, 50−56.
(35) Kong, X.; Shan, M.; Terskikh, V.; Hung, I.; Gan, Z.; Wu, G. Solid-State ^{17}O NMR of Pharmaceutical Compounds: Salicyclic Acid and Aspirin. *J. Phys. Chem. B* **2013**, *117*, 9643−9654.
(36) Kwan, I.; Mo, X.; Wu, G. Probing hydrogen bonding and ion-carbonyl interactions by solid-state ^{17}O NMR Spectroscopy: G-Ribbon and G-Quartet. *J. Am. Chem. Soc.* **2007**, *129*, 2398−2407.
(37) Wu, G. Solid-State ^{17}O NMR studies of organic and biological molecules: Recent advances and future directions. *Solid State Nucl. Magn. Reson.* **2016**, *73*, 1−14.
(38) Zhu, J. F.; Ye, E.; Terskikh, V.; Wu, G. Solid-State ^{17}O NMR Spectroscopy of Large Protein-Ligand Complexes. *Angew. Chem., Int. Ed.* **2010**, *49*, 8399−8402.
(39) Antzutkin, O. N.; Iuga, D.; Filippov, A. V.; Kelly, R. T.; Becker-Baldus, J.; Brown, S. P.; Dupree, R. Hydrogen Bonding in Alzheimer's Amyloid-β Fibrils Probed by ^{15}N{^{17}O} REAPDOR Solid-State NMR Spectroscopy. *Angew. Chem., Int. Ed.* **2012**, *124*, 10435−10438.
(40) Frydman, L.; Hardwood, J. S. Isotropic Spectra of Half-Integer Quadrupolar Spins from Bidimenstional Magic-Angle Spinning NMR. *J. Am. Chem. Soc.* **1995**, *117*, 5367−5368.
(41) Gan, Z. Isotropic NMR Spectra of Half-Integer Quadrupolar Nuclei Using Satellite Transitions and Magic-Angle Spinning. *J. Am. Chem. Soc.* **2000**, *122*, 3242−3243.
(42) Wu, G.; Rovnyak, D.; Huang, P. C.; Griffin, R. G. High-resolution oxygen-17 NMR spectroscopy of solids by multiple-quantum magic-angle-spinning. *Chem. Phys. Lett.* **1997**, *277*, 79−83.
(43) Wu, G.; Rovnyak, D.; Griffin, R. G. Quantitative multiple-quantum magic-angle-spinning NMR spectroscopy of quadrupolar nuclei in solids. *J. Am. Chem. Soc.* **1996**, *118*, 9326−9332.
(44) Wong, A.; Howes, A. P.; Yates, J. R.; Watts, A.; Anupõld, T.; Past, J.; Samoson, A.; Dupree, R.; Smith, M. E. Ultra-High Resolution ^{17}O Solid-State NMR Spectroscopy of Biomolecules: A Comprehensive Spectral Analysis of Monosodium L-Glutamate Monohydrate. *Phys. Chem. Chem. Phys.* **2011**, *13*, 12213−12224.
(45) O'Dell, L. A.; Ratcliffe, C. I.; Kong, X.; Wu, G. Multinuclear Solid-State Nuclear Magnetic Resonance and Density Functional Theory Characterization of Interaction Tensors in Taurine. *J. Phys. Chem. A* **2012**, *116*, 1008−1014.
(46) Prasad, S.; Clark, T. M.; Sharma, R.; Kwak, H. T.; Grandinetti, P. J.; Zimmermann, H. A Combined ^{17}O RAPT and MQ-MAS NMR Study of L-Leucine. *Solid State Nucl. Magn. Reson.* **2006**, *29*, 119−124.
(47) Keeler, E. G.; Michaelis, V. K.; Colvin, M. T.; Hung, I.; Gor'kov, P. L.; Cross, T. A.; Gan, Z.; Griffin, R. G. ^{17}O MAS NMR Correlation Spectroscopy at High Magnetic Fields. *J. Am. Chem. Soc.* **2017**, *139*, 17953−17963.
(48) Ashbrook, S. E. Recent advances in solid-state NMR spectroscopy of quadrupolar nuclei. *Phys. Chem. Chem. Phys.* **2009**, *11*, 6892−6905.
(49) Ashbrook, S. E.; Antonijevic, S.; Berry, A. J.; Wimperis, S. Motional broadening: an important distinction between multiple-quantum and satellite-transition MAS NMR of quadrupolar nuclei. *Chem. Phys. Lett.* **2002**, *364*, 634−642.
(50) Ashbrook, S. E.; Berry, A. J.; Frost, D. J.; Gregorovic, A.; Pickard, C. J.; Readman, J. E.; Wimperis, S. ^{17}O and ^{29}Si NMR parameters of $MgSiO_3$ phases from high-resolution solid-state NMR spectroscopy and first-principles calculations. *J. Am. Chem. Soc.* **2007**, *129*, 13213−13224.
(51) Ashbrook, S. E.; Berry, A. J.; Wimperis, S. Three- and five-quantum O-17 MAS NMR of forsterite Mg_2SiO_4. *Am. Mineral.* **1999**, *84*, 1191−1194.
(52) Ashbrook, S. E.; Berry, A. J.; Wimperis, S. ^{17}O multiple-quantum MAS NMR study of high-pressure hydrous magnesium silicates. *J. Am. Chem. Soc.* **2001**, *123*, 6360−6366.
(53) Ashbrook, S. E.; Berry, A. J.; Wimperis, S. ^{17}O multiple-quantum MAS NMR study of pyroxenes. *J. Phys. Chem. B* **2002**, *106*, 773−778.
(54) Dirken, P. J.; Kohn, S. C.; Smith, M. E.; van Eck, E. R. H. Complete resolution of Si-O-Si and Si-O-Al fragments in an aluminosilicate glass by ^{17}O multiple quantum magic angle spinning NMR spectroscopy. *Chem. Phys. Lett.* **1997**, *266*, 568−574.
(55) Stebbins, J. F.; Oglesby, J. V.; Lee, S. K. Oxygen sites in silicate glasses: a new view from oxygen-17 NMR. *Chem. Geol.* **2001**, *174*, 63−75.
(56) van Eck, E. R. H.; Smith, M. E.; Kohn, S. C. Observation of hydroxyl groups by ^{17}O solid-state multiple quantum MAS NMR in sol-gel-produced silica. *Solid State Nucl. Magn. Reson.* **1999**, *15*, 181−188.
(57) Lee, S. K.; Stebbins, J. F.; Weiss, C. A.; Kirkpatrick, R. J. ^{17}O and ^{27}Al MAS and 3QMAS NMR study of synthetic and natural layer silicates. *Chem. Mater.* **2003**, *15*, 2605−2613.
(58) Lee, S. K.; Weiss, C. A. Multiple oxygen sites in synthetic phyllosilicates with expandable layers: ^{17}O solid-state NMR study. *Am. Mineral.* **2008**, *93*, 1066−1071.
(59) Keeler, E. G.; Michaelis, V. K.; Griffin, R. G. ^{17}O NMR Investigation of Water Structure and Dynamics. *J. Phys. Chem. B* **2016**, *120*, 7851−7858.
(60) Michaelis, V. K.; Keeler, E. G.; Ong, T.-C.; Craigen, K. N.; Penzel, S. A.; Wren, J. E. C.; Kroeker, S.; Griffin, R. G. Structural Insights into Bound Water in Crystalline Amino Acids: Experimental and Theoretical ^{17}O NMR. *J. Phys. Chem. B* **2015**, *119*, 8024−8036.
(61) Anderson, M. R.; Jenkin, G. T.; White, J. W. Neutron-Diffraction Study of Lanthanum Magnesium-Nitrate $La_2Mg_3(NO_3)_{12}\cdot 24H_2O$. *Acta Crystallogr., Sect. B: Struct. Sci.* **1977**, *33*, 3933−3936.
(62) Gan, Z.; Hung, I.; Wang, X.; Paulino, J.; Wu, G.; Litvak, I. M.; Gor'kov, P. L.; Brey, W. W.; Lendi, P.; Schiano, J. L.; et al. NMR spectroscopy up to 35.2T using a series-connected hybrid magnet. *J. Magn. Reson.* **2017**, *284*, 125−136.
(63) Harris, R. K.; Becker, E. D.; De Menezes, S. M. C.; Granger, P.; Hoffman, R. E.; Zilm, K. W. Further conventions for NMR shielding and chemical shifts (IUPAC recommendations 2008). *Pure Appl. Chem.* **2008**, *80*, 59−84.
(64) Eichele, K. WSolids1 NMR Simulation Package, 1.20.21, 2013.
(65) Massiot, D.; Fayon, F.; Capron, M.; King, I.; Le Calve, S.; Alonso, B.; Durand, J. O.; Bujoli, B.; Gan, Z. H.; Hoatson, G. Modelling one- and two-dimensional solid-state NMR spectra. *Magn. Reson. Chem.* **2002**, *40*, 70−76.
(66) Bak, M.; Rasmussen, J. T.; Nielsen, N. C. SIMPSON: A general simulation program for solid-state NMR spectroscopy. *J. Magn. Reson.* **2000**, *147*, 296−330.
(67) Sternberg, U. The bond angle dependence of the asymmetry parameter of the oxygen-17 electric field gradient tensor. *Solid State Nucl. Magn. Reson.* **1993**, *2*, 181−190.
(68) Chiba, T. Deuteron Magnetic Resonance Study of Barium Chlorate Monohydrate. *J. Chem. Phys.* **1963**, *39*, 947−953.
(69) Thaper, C. L.; Dasannacharya, B. A.; Sequeira, A.; Iyengar, P. K. Observation of Librational Modes of Water Molecules in Single Crystal Hydrates by Neutron Scattering. *Solid State Commun.* **1970**, *8*, 497−499.
(70) Long, J. R.; Ebelhauser, R.; Griffin, R. G. ^{2}H NMR line shapes and spin-lattice relaxation in $Ba(ClO_3)_2\bullet{}^{2}H_2O$. *J. Phys. Chem. A* **1997**, *101*, 988−994.
(71) Perras, F. A.; Chaudhary, U.; Slowing, I. I.; Pruski, M. Probing Surface Hydrogen Bonding and Dynamics by Natural Abundance, Multidimensional, ^{17}O DNP-NMR Spectroscopy. *J. Phys. Chem. C* **2016**, *120*, 11535−11544.

DOI: 10.1021/acs.jpcb.9b02277
J. Phys. Chem. B 2019, 123, 3061−3067

(72) Perras, F. A.; Kobayashi, T.; Pruski, M. Natural Abundance ^{17}O DNP Two-Dimensional and Surface-Enhanced NMR Spectroscopy. *J. Am. Chem. Soc.* **2015**, *137*, 8336−8339.
(73) Hung, I.; Uldry, A. C.; Becker-Baldus, J.; Webber, A. L.; Wong, A.; Smith, M. E.; Joyce, S. A.; Yates, J. R.; Pickard, C. J.; Dupree, R.; et al. Probing Heteronuclear ^{15}N-^{17}O and ^{13}C-^{17}O Connectivities and Proximities by Solid-State NMR Spectroscopy. *J. Am. Chem. Soc.* **2009**, *131*, 1820−1834.
(74) Carnahan, S. L.; Lampkin, B. J.; Naik, P.; Hanrahan, M. P.; Slowing, I. I.; VanVeller, B.; Wu, G.; Rossini, A. J. Probing O-H Bonding Through Proton Detected ^{1}H-^{17}O Double Resonance Solid-State NMR Spectroscopy. *J. Am. Chem. Soc.* **2018**, *141*, 441−450.
(75) Michaelis, V. K.; Corzilius, B.; Smith, A. A.; Griffin, R. G. Dynamic Nuclear Polarization of ^{17}O: Direct Polarization. *J. Phys. Chem. B* **2013**, *117*, 14894−14906.
(76) Michaelis, V. K.; Markhasin, E.; Daviso, E.; Herzfeld, J.; Griffin, R. G. Dynamic Nuclear Polarization of Oxygen-17. *J. Phys. Chem. Lett.* **2012**, *3*, 2030−2034.

DOI: 10.1021/acs.jpcb.9b02277
J. Phys. Chem. B 2019, 123, 3061−3067